THE JOURNAL OF BIOLOGICAL CHEMISTRY VOL. 285, NO. 3, pp. 2040–2050, January 15, 2010

Mitochondrial Ca^{2+} Uptake Increases Ca^{2+} Release from Inositol 1,4,5-Trisphosphate Receptor Clusters in Smooth Muscle Cells*

Received for publication, May 29, 2009, and in revised form, October 16, 2009 Published, JBC Papers in Press, November 4, 2009, DOI 10.1074/jbc.M109.027094

Marnie L. Olson, Susan Chalmers, and John G. McCarron[1]

From the Strathclyde Institute of Pharmacy and Biomedical Sciences, University of Strathclyde, John Arbuthnott Building, Glasgow G4 0NR, Scotland, United Kingdom

Smooth muscle activities are regulated by inositol 1,4,5-trisphosphate ($InsP_3$)-mediated increases in cytosolic Ca^{2+} concentration ($[Ca^{2+}]_c$). Local Ca^{2+} release from an $InsP_3$ receptor ($InsP_3R$) cluster present on the sarcoplasmic reticulum is termed a Ca^{2+} puff. Ca^{2+} released via $InsP_3R$ may diffuse to adjacent clusters to trigger further release and generate a cell-wide (global) Ca^{2+} rise. In smooth muscle, mitochondrial Ca^{2+} uptake maintains global $InsP_3$-mediated Ca^{2+} release by preventing a negative feedback effect of high $[Ca^{2+}]$ on $InsP_3R$. Mitochondria may regulate $InsP_3$-mediated Ca^{2+} signals by operating between or within $InsP_3R$ clusters. In the former mitochondria could regulate only global Ca^{2+} signals, whereas in the latter both local and global signals would be affected. Here whether mitochondria maintain $InsP_3$-mediated Ca^{2+} release by operating within (local) or between (global) $InsP_3R$ clusters has been addressed. Ca^{2+} puffs evoked by localized photolysis of $InsP_3$ in single voltage-clamped colonic smooth muscle cells had amplitudes of 0.5–4.0 F/F_0, durations of ~112 ms at half-maximum amplitude, and were abolished by the $InsP_3R$ inhibitor 2-aminoethoxydiphenyl borate. The protonophore carbonyl cyanide 3-chloropheylhydrazone and complex I inhibitor rotenone each depolarized $\Delta\Psi_M$ to prevent mitochondrial Ca^{2+} uptake and attenuated Ca^{2+} puffs by ~66 or ~60%, respectively. The mitochondrial uniporter inhibitor, RU360, attenuated Ca^{2+} puffs by ~62%. The "fast" Ca^{2+} chelator 1,2-bis(*o*-aminophenoxy)ethane-*N*,*N*,*N*′,*N*′-tetraacetic acid acted like mitochondria to prolong $InsP_3$-mediated Ca^{2+} release suggesting that mitochondrial influence is via their Ca^{2+} uptake facility. These results indicate Ca^{2+} uptake occurs quickly enough to influence $InsP_3R$ communication at the intra-cluster level and that mitochondria regulate both local and global $InsP_3$-mediated Ca^{2+} signals.

Smooth muscle functions to regulate many activities including blood flow in vascular blood vessels, peristaltic motion in the gastrointestinal tract, and rhythmic contractions of the uterus during labor. Transient increases in the cytosolic Ca^{2+} concentration ($[Ca^{2+}]_c$)[2] provides the major trigger for contraction to regulate these activities. Other smooth muscle cell functions are also regulated by Ca^{2+} including transcription, growth, and apoptosis. Stimuli acting on the cell may increase $[Ca^{2+}]_c$ by influx of the ion from the extracellular medium, release from intracellular stores or both. The sarcoplasmic reticulum (SR) is an intracellular Ca^{2+} storage organelle and contains two Ca^{2+} release channels, the ryanodine receptor (RyR) and the inositol 1,4,5-trisphosphate receptor ($InsP_3R$). Release from RyR is triggered by a small influx of Ca^{2+} across the plasma membrane in a process known as Ca^{2+}-induced Ca^{2+}-release, which occurs in cardiac and skeletal muscle or in smooth muscle when the SR contains excessive levels of Ca^{2+} (1–3). In non-contracting cell types and smooth muscle, Ca^{2+} release from the SR occurs predominantly via $InsP_3R$ and is triggered by hormonal stimulation of G protein-coupled receptors.

$InsP_3R$ are not distributed uniformly throughout the SR but exist as clusters composed typically of 25–60 channels (4, 5). Ca^{2+} release from a cluster of $InsP_3R$, a Ca^{2+} puff, is attributed to the activation of a small number of $InsP_3R$ within the cluster (4, 5). Ca^{2+} puffs are spatially localized Ca^{2+} transients that are short in duration and are considered the elementary building blocks of Ca^{2+} release from $InsP_3R$ (6–10). Ca^{2+} puffs have been observed in several cell types including *Xenopus* oocytes, rat basophilic leukemia, glial, PC12, and smooth muscle cells where the localized release forms microdomains of $[Ca^{2+}]_c$, which exceed that of the bulk cytoplasm (6–8, 10–12). Propagation of the Ca^{2+} response through the cell occurs when Ca^{2+} released from one $InsP_3R$ cluster diffuses to other neighboring clusters and, in the presence of $InsP_3$, activates them in a Ca^{2+}-induced Ca^{2+}-release-like process (7, 8, 13, 14). Thus, activation of $InsP_3R$ may generate a variety of Ca^{2+} responses that include localized Ca^{2+} puffs or cell-wide (global) responses in the form of Ca^{2+} oscillations and propagating Ca^{2+} waves.

Mitochondria, in addition to their ATP generating facility, take up Ca^{2+} from the cytosol. Global $InsP_3$-mediated Ca^{2+} release is modulated by mitochondrial Ca^{2+} uptake in smooth muscle and other cell types, which include HeLa cells, *Xenopus* oocytes, PC12 cells, and cultured oligodendrocytes (15–20).

* This work was supported by Wellcome Trust Grant 078054/Z/05/Z and British Heart Foundation Grant PG/08/066.

[1] To whom correspondence should be addressed. Tel.: 44-141-548-4119; Fax: 44-141-552-2562; E-mail: john.mccarron@strath.ac.uk.

[2] The abbreviations used are: $[Ca^{2+}]_c$, cytosolic Ca^{2+} concentration; $InsP_3$, inositol 1,4,5-trisphosphate; $InsP_3R$, inositol 1,4,5-trisphosphate receptor; $\Delta\Psi_M$, mitochondrial membrane potential; SR, sarcoplasmic reticulum; RyR, ryanodine receptor; $[Ca^{2+}]_{mit}$, mitochondrial Ca^{2+} concentration; AM, acetoxymethylester; CCCP, carbonyl cyanide 3-chloropheylhydrazone; FWHD, duration at half-maximum amplitude; 2-APB, 2-aminoethoxydiphenyl borate; TMRE, tetramethylrhodamine ethyl ester; BAPTA, 1,2-bis(*o*-aminophenoxy)ethane-*N*,*N*,*N*′,*N*′-tetraacetic acid.

Mitochondrial Ca^{2+} uptake and the increase in mitochondrial Ca^{2+} concentration ($[Ca^{2+}]_{mit}$), which normally occurs during global $InsP_3$-mediated increases in $[Ca^{2+}]_c$ is prevented by depolarizing the mitochondrial membrane potential ($\Delta\Psi_M$) in HeLa and rat basophilic leukemia-2H3 mast cells (21, 22). Inhibition of mitochondrial Ca^{2+} uptake has various effects on global $InsP_3$-mediated Ca^{2+} release. Mitochondrial Ca^{2+} uptake may negatively regulate $InsP_3$-mediated Ca^{2+} release in cultured hepatocytes and astrocytes. Here the Ca^{2+} wave amplitude or velocity or both increased when mitochondrial Ca^{2+} uptake was prevented by depolarizing $\Delta\Psi_M$ (23, 24). In other cell types mitochondrial Ca^{2+} uptake positively affects $InsP_3$-mediated Ca^{2+} release so that preventing uptake inhibited Ca^{2+} responses in smooth muscle, astrocytes, and HeLa cells and increasing mitochondrial Ca^{2+} uptake augmented $InsP_3$-mediated Ca^{2+} wave amplitude and velocity in *Xenopus* oocytes (15–17, 19, 20, 25).

The differences in mitochondrial regulation of global $InsP_3$-mediated Ca^{2+} release in various tissues may arise from the localization of sites of mitochondrial Ca^{2+} uptake relative to sites of SR Ca^{2+} release. Proximity of sites of mitochondrial Ca^{2+} uptake to $InsP_3R$ clusters may determine whether Ca^{2+} uptake prevents either inactivation or complete activation of $InsP_3R$. The localization of mitochondria will also determine whether the organelle may only regulate the global signal (*e.g.* waves) alone or may additionally regulate local (*e.g.* puffs) Ca^{2+} signals. For example, localization of mitochondria between $InsP_3R$ clusters will enable the organelle to regulate global but not local Ca^{2+} signals. On the other hand, mitochondria positioned at $InsP_3R$ clusters will enable the organelle to regulate local and global Ca^{2+} signals. To determine whether mitochondria regulate local or global Ca^{2+} signals, the effect of depolarizing $\Delta\Psi_M$, or inhibiting the mitochondrial uniporter, to prevent mitochondrial Ca^{2+} uptake, on localized release of Ca^{2+} from $InsP_3R$ clusters (Ca^{2+} puffs) has been examined. $InsP_3$-mediated Ca^{2+} puffs were evoked by localized flash photolysis of caged $InsP_3$ in colonic smooth muscle cells. Ca^{2+} puff sites were uncoupled by using EGTA to prevent Ca^{2+} release from one $InsP_3R$ cluster activating adjacent $InsP_3R$ clusters and generate a global Ca^{2+} wave. Inhibition of mitochondrial Ca^{2+} uptake attenuated the magnitude of Ca^{2+} puffs as well as global $InsP_3$-mediated Ca^{2+} signals. These results indicate that mitochondrial Ca^{2+} uptake influences the $InsP_3R$ communication at the intra-cluster level by regulating the amount of Ca^{2+} released from a cluster of $InsP_3R$ before the released Ca^{2+} diffuses between $InsP_3R$ clusters. Mitochondrial Ca^{2+} uptake appears to prevent a negative feedback effect of high $[Ca^{2+}]_c$ on $InsP_3R$ activity within a cluster to prolong Ca^{2+} release from the SR. Support for this conclusion was found in experiments which show the "fast" Ca^{2+} chelator 1,2-bis(*o*-aminophenoxy)ethane-*N*,*N*,*N*′,*N*′-tetraacetic acid (BAPTA) also prolonged Ca^{2+} release via $InsP_3R$ clusters. Together, these results indicate that sites of mitochondrial Ca^{2+} uptake are located in proximity to $InsP_3R$ to influence the local and global response to $InsP_3$-mediated Ca^{2+} release.

EXPERIMENTAL PROCEDURES

Cell Isolation—Male guinea pigs (350–500 g) were humanely killed by cervical dislocation followed by immediate exsanguination in accordance with the guidelines of the Animal (Scientific Procedures) Act UK 1986. A segment of intact distal colon (~5 cm) was transferred to oxygenated (95% O_2, 5% CO_2) physiological saline solution comprising (mM): 118.4 NaCl, 25 $NaHCO_3$, 4.7 KCl, 1.13 NaH_2PO_4, 1.3 $MgCl_2$, 2.7 $CaCl_2$, and 11 glucose (pH 7.4). Following removal of the mucosa and longitudinal muscle layer from the tissue, single smooth muscle cells, largely from circular muscle, were enzymatically dissociated (16). All experiments were carried out at room temperature (20 ± 2 °C).

Electrophysiology—Cells were voltage-clamped using conventional tight-seal whole cell recording methods (26). The extracellular solution contained (mM): 80 sodium glutamate, 40 NaCl, 20 tetraethylammonium chloride, 1.1 $MgCl_2$, 3 $CaCl_2$, 10 HEPES, and 30 glucose (pH 7.4 with NaOH). The pipette solution contained (mM): 85 Cs_2SO_4, 20 CsCl, 1 $MgCl_2$, 30 HEPES, 3 MgATP, 2.5 pyruvic acid, 2.5 malic acid, 1 NaH_2PO_4, 5 creatine phosphate, 0.5 guanosine phosphate, and 0.025 caged inositol 1,4,5-trisphosphate ($InsP_3$) trisodium salt. Pyruvic acid and malic acid were present to maintain mitochondrial activity. The high concentration of HEPES was to ensure pH control during mitochondrial depolarization. Creatine phosphate and ATP were to maintain [ATP] during the experiments. Whole cell currents were measured using an Axopatch 200B (Axon Instruments, Union City, CA), low-pass filtered at 500 Hz (8-pole Bessel filter; Frequency Devices, Haverhill, MA), digitally sampled at 1.5 kHz using a Digidata interface and pClamp (version 8; Axon Instruments) and stored for analysis. In the majority of experiments, as specified under "Results," EGTA (250 μM to 1 mM) was added to the pipette solution to buffer the $[Ca^{2+}]_c$. EGTA was added to uncouple $InsP_3R$ clusters (27). The slow binding kinetics (K_{on} = ~5 $\mu M^{-1}\ s^{-1}$) of the buffer prevents EGTA from significantly influencing the release of Ca^{2+} within a cluster (28). In other experiments, as specified under "Results," BAPTA (250 μM) replaced EGTA in the pipette solution to buffer the $[Ca^{2+}]_c$. The fast binding kinetics of BAPTA (K_{on} = 100–1000 $\mu M^{-1}\ s^{-1}$) influences Ca^{2+} release within an $InsP_3R$ cluster (28).

Imaging—Single, freshly isolated colonic smooth muscle cells were loaded with the Ca^{2+}-sensitive dye fluo 3 acetoxymethylester (AM) (10 μM) and wortmannin (10 μM; to prevent contraction) for at least 20 min before the start of the experiment and then allowed to settle for 10 min. 30 min was sufficient to allow intracellular esterases to hydrolyze the AM moiety. Two-dimensional $[Ca^{2+}]_c$ images were obtained using a wide-field digital imaging system. Single cells were illuminated at 488 nm (bandpass 14 nm) from a monochrometer (Polychrome IV, T.I.L.L. Photonics, Martinsried, Germany) and imaged through an oil-immersion objective (×40 UV 1.3 NA; Nikon UK, Surrey, United Kingdom). Excitation light was passed via a fiber optic guide through a 485-bandpass (15 nm) filter and a fieldstop diaphragm and reflected off a 505-nm long-pass dichroic mirror. Emitted light was guided through a 535-nm barrier filter (bandpass 45 nm) to an intensified,

cooled, frame transfer CCD camera (Pentamax Gen IV, Roper Scientific, Trenton, NJ) operating in "virtual chip" mode with program WinView 32 (Roper Scientific, Trenton, NJ). Full-frame images (160 × 160 pixels), with a pixel size of 720 nm at the cell, were acquired at 50 frames/s. In some experiments the software program Metafluor (Molecular Devices, Wokingham, UK) was used to obtain longer periods of data acquisition. In these experiments sampling rates of ~10 frames/s were used during and 1 frame/s between Ca^{2+} transients. Ca^{2+} imaging data were recorded on a personal computer. Electrophysiological measurements and imaging data were synchronized by recording, on pClamp, a transistor transistor logic output from the CCD camera, which reported its readout status together with the electrophysiological information.

In some experiments, cells were loaded with the Ca^{2+}-sensitive dye fluo 4-AM (10 μM) and the $\Delta\Psi_M$-sensitive dye tetramethylrhodamine ethyl ester (TMRE) (10 nM) so that $[Ca^{2+}]_i$ and $\Delta\Psi_M$, respectively, could be imaged near simultaneously (15). Here cells were illuminated at 475 and 560 nm, respectively, and light was passed via a fiber optic guide through a dual 483/553-nm bandpass filter (bandpass 15 and 20 nm, respectively), through an ND4 neutral density filter, and reflected off a custom-made dual long-pass dichroic mirror (transmissive in ranges 505–540 and 577–640 nm, and reflective from 490 to below 300 nm; Chroma, Rockingham, VT). The emitted light was guided through a dual bandpass 518/594-nm barrier filter (bandpass 25 and 18 nm, respectively) to the CCD camera.

Localized Flash Photolysis—The output of a xenon flashlamp (Rapp Optoelecktronic, Hamburg, Germany), used to uncage $InsP_3$, was passed through a UG-5 filter to select ultraviolet light, focused, and merged into the excitation light path through a fiber optic bundle and long-pass dichroic mirror at the lens part of the epi-illumination attachment of the microscope. The diameter of the fiber optic together with the lens magnification determined the area (spot size ~20 or ~125 μm) of $InsP_3$ photolysis (29). A photolysis region of ~20 μm diameter was used to evoke $InsP_3$-mediated Ca^{2+} release to allow for greater flexibility in photolysis spot placement relative to the patch clamp electrode to prevent uncaging of $InsP_3$ within the patch pipette. The output intensity of the flash lamp was altered in the Ca^{2+} puff experiments to between 20 and 100% (0.025–0.19 milliwatts) of the maximum output to control the amount of $InsP_3$ that was uncaged and determined empirically in each cell.

Data Analysis—Images were analyzed using the program Metamorph 7.1.3 (Molecular Devices, Wokingham, UK). Fluorescence images were initially background subtracted and smoothed using a median average of 3 × 3 pixels. Changes in fluorescence were expressed as ratios (F/F_0 or $\Delta F/F_0$) of fluorescence counts (F) relative to baseline (control) values (taken as 1) before stimulation (F_0). The average baseline value over the 100 frames occurring before flash photolysis of caged $InsP_3$ was subtracted from peak height ($\Delta F/F_0$). Full width at half-maximum amplitude (FWHD) was used to determine the duration of the puff at half its peak value. The time to peak of the Ca^{2+} puff was measured as the time required to increase from 10 to 90% of maximal peak amplitude. The decay of the Ca^{2+} puff was measured as the time required to decline from 90 to 10% of maximal amplitude. The delay in the onset of the Ca^{2+} puff after photolysis of $InsP_3$ was measured as the time required for $[Ca^{2+}]_c$ to increase by 0.2 F/F_0 from baseline values.

Summarized results are expressed as mean ± S.E. of n cells. A paired or unpaired Student's t test was applied to the raw data, as appropriate; $p < 0.05$ was considered significant.

Drugs and Chemicals—Drugs were applied by addition to the extracellular solution. Concentrations in the text refer to the salts, where appropriate. Fluo 3-AM, fluo 4-AM, and TMRE were purchased from Invitrogen and caged $InsP_3$-trisodium salt from SiChem GmbH (Bremen, Germany). All other reagents were purchased from Sigma.

RESULTS

In voltage-clamped, single smooth muscle cells flash photolysis of caged $InsP_3$ (25 μM) at 60-s intervals produced transient elevations in the free intracellular Ca^{2+} concentration ($[Ca^{2+}]_c$) throughout the photolysis region (*i.e.* global increases) (Fig. 1). Upon photolysis of $InsP_3$, $[Ca^{2+}]_c$, measured by $\Delta F/F_0$, increased to 3.91 ± 0.63 ($n = 6$). The rise in $[Ca^{2+}]_c$ from $InsP_3$ occurs exclusively as a result of $InsP_3R$ activity; $InsP_3$-mediated Ca^{2+} release does not activate further Ca^{2+} release via RyR (30, 31).

Mitochondria accumulate Ca^{2+} in these cells following release of the ion via IP_3R (15). The contribution of mitochondrial Ca^{2+} uptake to the magnitude of global $InsP_3$-mediated SR Ca^{2+} release was examined. Mitochondrial Ca^{2+} uptake was prevented by collapsing the mitochondrial electrochemical ($\Delta\Psi_M$) gradient using the protonophore CCCP. Because, in CCCP, the mitochondrial ATPase operates in reverse direction oligomycin was also included to inhibit the F_1F_0-ATPase and prevent ATP depletion. ATP (3 mM) and phosphocreatine (5 mM) were present in the patch pipette filling solution. When mitochondrial Ca^{2+} uptake was prevented in CCCP and oligomycin (1 and 6 μM, respectively), the $InsP_3$-mediated Ca^{2+} increase was inhibited (see Fig. 1) (15, 16). The $InsP_3$-mediated Ca^{2+} increase was 3.91 ± 0.63 $\Delta F/F_0$ in control and 1.33 ± 0.47 $\Delta F/F_0$ ($n = 6$) after CCCP and oligomycin (*i.e.* 34% of control ($p < 0.05$)). The inhibition of the IP_3-mediated Ca^{2+} release is unlikely to be explained by a reduction in the SR Ca^{2+} content by CCCP and oligomycin. The SR Ca^{2+} content, as assessed by the extent of Ca^{2+} release by the RyR agonist caffeine was unaffected by CCCP plus oligomycin (Fig. 1*D*). RyR and IP_3R share access to a single common Ca^{2+} store in these cells (32). Together, mitochondrial Ca^{2+} uptake regulates global $InsP_3$-mediated Ca^{2+} release.

To generate a global increase in Ca^{2+}, Ca^{2+} released via one cluster of $InsP_3R$ activates other adjacent $InsP_3R$ clusters in a Ca^{2+}-induced Ca^{2+}-release-like manner to summate into a cell-wide Ca^{2+} rise (8, 33, 34). Mitochondria may control the global rise in $[Ca^{2+}]_c$ evoked by $InsP_3$ by regulating the Ca^{2+} signal that propagates among $InsP_3R$ clusters. Alternatively mitochondria may regulate the Ca^{2+} signal, which occurs within a single $InsP_3R$ cluster. In the former, mitochondria may only regulate global Ca^{2+} signals. In the latter, both local and global signals will be controlled by mitochondrial activity. The question arises do mitochondria influence $InsP_3$-mediated release by operating within or between $InsP_3R$ clusters?

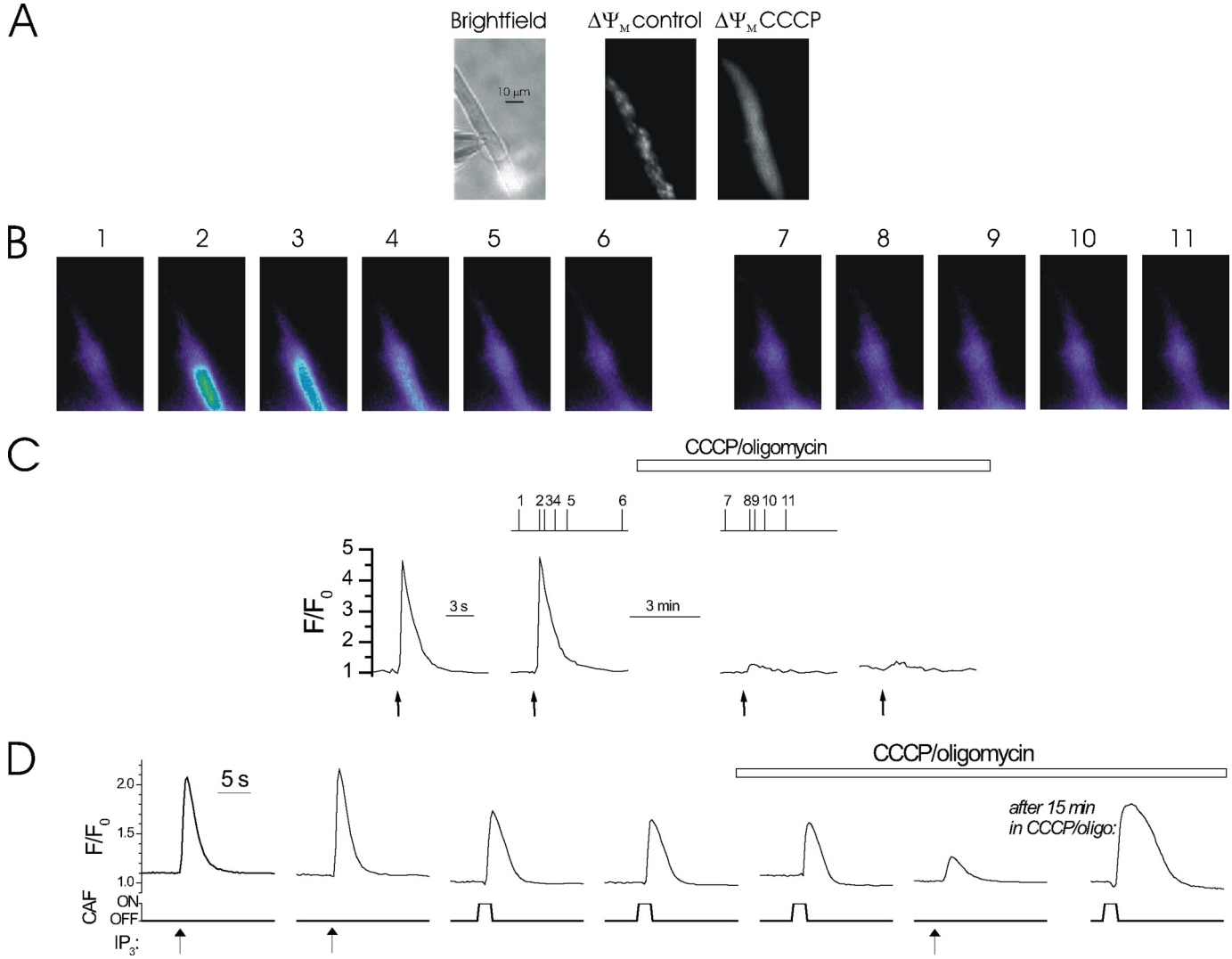

FIGURE 1. **Mitochondrial depolarization decreased the magnitude of InsP$_3$-mediated Ca^{2+} release.** At −70 mV, locally photolyzed caged InsP$_3$ (25 μM) (↑, *C*) in a ~20 μm diameter region (*A, bright spot* in *left-hand panel*, see also whole cell electrode, *left side*) evoked approximately reproducible rises in Ca^{2+} in a freshly isolated colonic myocyte (*B* and *C*). Depolarization of $\Delta\Psi_M$ by the protonophore CCCP (1 μm) (used with oligomycin; 6 μm) inhibited InsP$_3$-mediated Ca^{2+} increases (*B* and *C*). $[Ca^{2+}]_c$ and $\Delta\Psi_M$ are shown near simultaneously using fluo 4 and TMRE, respectively. Mitochondria appeared as punctuate areas of fluorescence because of their $\Delta\Psi_M$ and were imaged before (*A, middle panel*) and after (*A, right-hand panel*) superfusion of CCCP. When $\Delta\Psi_M$ was depolarized TMRE dissipated and redistributed throughout the cell. The $[Ca^{2+}]_c$ images (*B*) are derived from the time points indicated by the corresponding numbers in *C*. $[Ca^{2+}]_c$ changes in *B* are expressed by color; *dark blue,* low and *yellow,* high $[Ca^{2+}]_c$. Flash photolysis of InsP$_3$ (↑, *C*) at ~60-s intervals generated approximately comparable $[Ca^{2+}]_c$ increases (*C*). InsP$_3$ continued to be photolyzed at ~60-s intervals during superfusion of CCCP and oligomycin to depolarize $\Delta\Psi_M$, which inhibits mitochondrial Ca^{2+} uptake (*horizontal bar; C*). Measurements were made from a 3 × 3 pixel box located within the flash area. Mitochondrial depolarization with CCCP plus oligomycin did not alter SR Ca^{2+} content: RyR activation by caffeine (*CAF,* 100 μM, applied by localized pressure ejection) evoked comparable Ca^{2+} release before, immediately after, and 15 min after superfusion of CCCP plus oligomycin (1 and 6 μM, respectively), despite inhibition of Ca^{2+} increases evoked by InsP$_3$ (*D*).

To address this question, mitochondrial regulation of the amplitude and duration of Ca^{2+} release from a single cluster of InsP$_3$R was examined. Ca^{2+} puffs, the fluorescence manifestation of the discrete release of Ca^{2+} from a single cluster of InsP$_3$R, were evoked by low energy (~20–50% of maximum) flash photolysis of caged InsP$_3$ (25 μM). Ca^{2+} puffs differed from a global rise in $[Ca^{2+}]_c$ in that they were localized events that occurred within a small region of the flash area and their duration was much shorter than for a global release of Ca^{2+}. In contrast, when there was a global rise, $[Ca^{2+}]_c$ increased uniformly throughout the flash area. The following criteria identified Ca^{2+} rises as "puffs": a change in peak amplitude of between 1 and 3 $\Delta F/F_0$, time to peak of 50 to 100 ms, and a duration at half-maximum amplitude (FWHD) of 100 to 200 ms. These criteria are derived from those previously reported in smooth muscle, *Xenopus* oocytes, and HeLa cells (7, 10, 13, 14, 35).

In initial experiments Ca^{2+} puffs were observed infrequently and over only a narrow range of [InsP$_3$] above which they were rapidly summated to produce a global rise in Ca^{2+} response. To overcome this restricted range and evoke Ca^{2+} puffs consistently, a low concentration of the slow Ca^{2+} buffer, EGTA, was added to the cells via the patch pipette. EGTA prevents InsP$_3$-mediated Ca^{2+} puffs from coalescing into a global Ca^{2+} rise because the buffer prevents the ion from reaching neighboring InsP$_3$R clusters (27). As a first step in these experiments, the effect of [EGTA] (between 250 μM and 1 mM) on Ca^{2+} puffs was examined. At [EGTA] (250–500 μM) Ca^{2+} puffs of a similar

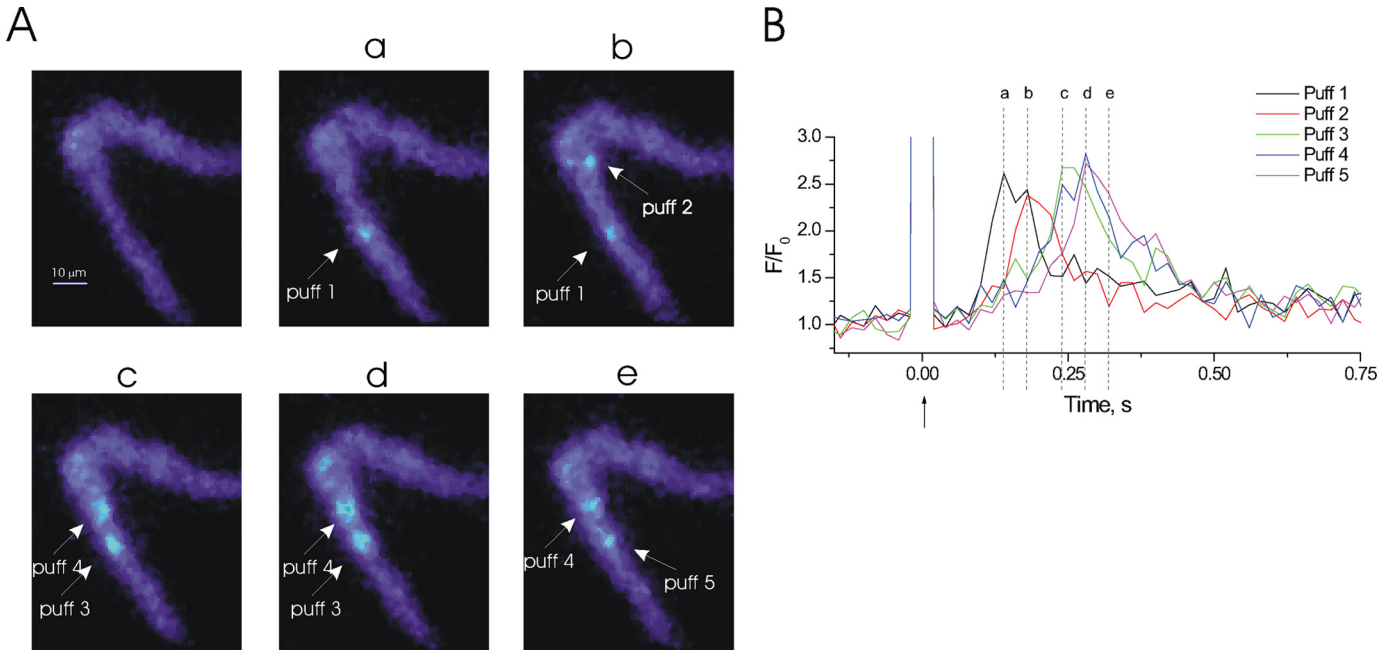

FIGURE 2. **Ca^{2+} puffs may occur with different latencies of onset after photolysis of $InsP_3$.** At −70 mV, localized photolysis of caged $InsP_3$ (25 μM) (↑, *B*) in a ~20-μm diameter region triggered several Ca^{2+} puffs (*A* and *B*). Five localized Ca^{2+} puffs were evoked within the photolysis site; the time of onset for each Ca^{2+} puff was variable. Ca^{2+} puff 1 occurred 160 ms after photolysis of $InsP_3$ and was located 22.5 μm away from Ca^{2+} puff 2, which occurred 200 ms after photolysis. The measurement of delay in Ca^{2+} puff onset after photolysis of $InsP_3$ was determined by how long it took for the $[Ca^{2+}]_c$ to increase by 0.2 F/F_0 from baseline. The $[Ca^{2+}]_c$ images (*A*) are derived from the time points indicated by the corresponding *lowercase letters* in *B*. $[Ca^{2+}]_c$ changes in *A* are expressed by color: *dark blue*, low and *light blue*, high $[Ca^{2+}]_c$. Measurements were made from 3 × 3 pixel boxes located at the center of each puff (not shown). To record Ca^{2+} puffs single colonic myocytes were buffered using EGTA (300 μM). This did not affect the amplitude, nor duration of the puff but did allow for puffs to be recorded using a larger range of concentrations of $InsP_3$. The large increase in fluorescence at time 0 is the flash artifact.

TABLE 1

Comparison of the amplitude, time to peak, full width at half-maximum amplitude, decay time, and latency of onset of Ca^{2+} puffs under different conditions

The time to peak and decay time were determined from the changes that occurred between 10 and 90% of the peak $\Delta F/F_0$ values.

Condition	Amplitude, $\Delta F/F_0$	Time to peak (10–90%)	FWHD	Decay time (90-10%)	Latency of onset	*n*
			ms			
EGTA buffered	1.94 ± 0.24	57 ± 8	112 ± 16	267 ± 40	64 ± 12	36 from 12 cells
BAPTA buffered	1.53 ± 0.54	1486 ± 156	1208 ± 334	4324 ± 435		12 from 4 cells
Not buffered	1.01 ± 0.17	419 ± 141	481 ± 76	1066 ± 279		3 from 3 cells

magnitude to those reported elsewhere and in non-buffered cells were measured (Fig. 2). Above 500 μM EGTA significantly attenuated the amplitude of Ca^{2+} puffs and, in some cells, they could not be evoked. EGTA (300 μM) at a concentration similar to that used in experiments examining Ca^{2+} puffs in *Xenopus* oocytes was used in the present study to enable Ca^{2+} puffs to be evoked and measured (27, 36). EGTA (300 μM) neither affects the magnitude nor slows the kinetics of Ca^{2+} puffs (27, 37).

Characteristics of Ca^{2+} Puffs—In each cell there were typically one to five individual puffs evoked within the photolysis region (~20 μm diameter). The latency between photolysis of caged $InsP_3$ and onset of the Ca^{2+} puff, peak amplitude, time to peak, FWHD, and decay time were measured (Table 1). The amplitude of Ca^{2+} puffs varied between 0.5 and 4.0 $\Delta F/F_0$ and averaged 1.94 ± 0.24 $\Delta F/F_0$ (n = 36 from 12 cells). The average time to peak (10–90% interval) of Ca^{2+} puffs was 57 ± 8 ms, FWHD was 112 ± 16 ms, and the decay time (90–10% interval) was 267 ± 40 ms. Ca^{2+} puffs also had variable latency between the time of photolysis of $InsP_3$ and when the rise in $[Ca^{2+}]_c$ occurred (Fig. 2). In the representative cell shown in Fig. 2, five Ca^{2+} puffs occurred after photolysis of $InsP_3$. Fig. 2*A*, *a* and *b*, show two Ca^{2+} puffs (*puff 1* and *puff 2*) that are 22.5 μm apart; the peak of Ca^{2+} puff 1 preceded that of puff 2 by 40 ms. The majority of cells analyzed displayed 1–2 puff sites and the average onset latency was ~64 ± 12 ms (n = 36 from 12 cells).

Ca^{2+} puffs at various sites were not of fixed and constant size but had a continuum of amplitudes presumably due to activation of a different number of $InsP_3R$ within different clusters (13, 38). In the representative cell shown in Fig. 3 a large photolysis region (125 μm diameter) was used to evoke $InsP_3$-mediated Ca^{2+} release and generated puffs of various amplitudes at different sites. There were three individual Ca^{2+} puffs (labeled *puff 1*, *2*, and *3*); the largest increase in $[Ca^{2+}]_c$ occurred at puff 2. The increases in $[Ca^{2+}]_c$, which occurred at the other sites are unlikely to be explained by diffusion of Ca^{2+} from puff 2 (Fig. 3, *B* and *C*). If the increases in $[Ca^{2+}]_c$ were due to diffusion, then a gradual decrease in the maximum change in $[Ca^{2+}]_c$ would be expected to have occurred from the site of Ca^{2+} release, the rate of Ca^{2+} increase would have decreased, and there would be a delay in the onset of the Ca^{2+} increase. At a location situated outside the flash site area, where $InsP_3$ was not photoreleased, no increase in $[Ca^{2+}]_c$ occurred (region 4).

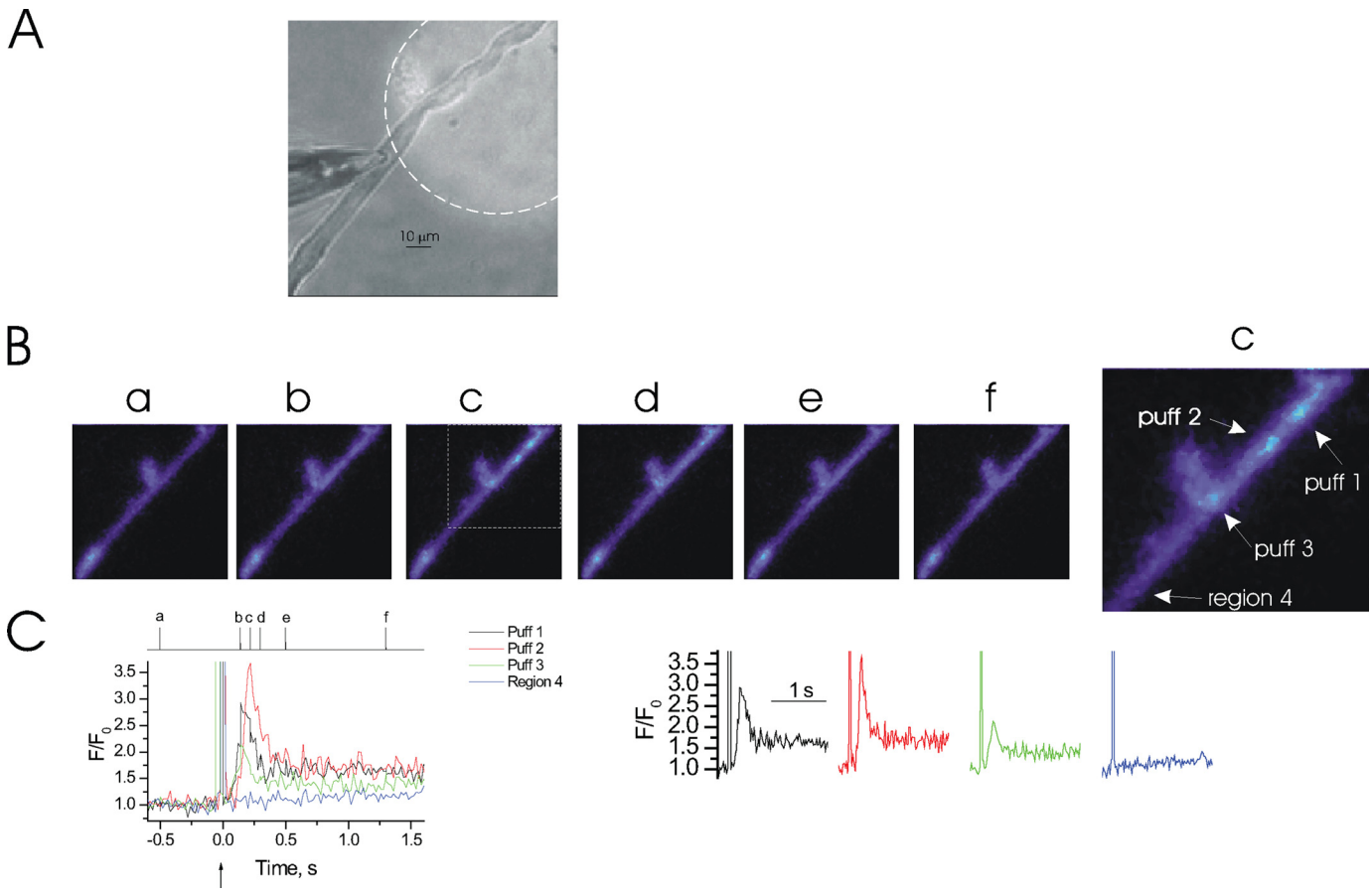

FIGURE 3. **InsP$_3$-mediated Ca^{2+} puffs may occur in multiple regions simultaneously.** At −70 mV, localized photolysis of caged InsP$_3$ (25 μM) (↑, *C*) in a 125-μm diameter region (*A*, *bright spot* highlighted with a *dotted line*, see also whole cell electrode, *left side*) triggered Ca^{2+} puffs in an EGTA (300 μM)-buffered colonic myocyte (*B* and *C*). The Ca^{2+} puffs were of various amplitudes and occurred near simultaneously in different regions of the flash photolysis site. $[Ca^{2+}]_c$ did not increase in areas (region 4) located outside the photolysis site. The $[Ca^{2+}]_c$ images (*B*) are derived from the time points indicated by the corresponding *lowercase letters* in *C*. $[Ca^{2+}]_c$ changes in *B* are expressed by color: *dark blue*, low and *light blue*, high $[Ca^{2+}]_c$. Measurements were made from 3 × 3 pixel boxes located at the center of each puff (not shown). The large increase in fluorescence at time 0 is the flash artifact.

Although puffs at different sites had various amplitudes, within a site Ca^{2+} puffs could be reproducibly evoked and had consistent amplitudes (see Figs. 5*C*, 6*C*, and 7*C*). In the remaining experiments a photolysis region of ~20 μm diameter was used to evoke InsP$_3$-mediated Ca^{2+} release to allow for greater flexibility in photolysis spot placement relative to the patch clamp electrode to prevent uncaging of InsP$_3$ within the patch pipette.

Ca^{2+} puffs could be evoked in the absence of the Ca^{2+} buffer EGTA. However, there was substantial variation in response to the same photolysis strength and Ca^{2+} puffs could only be evoked over a narrow range of [InsP$_3$] and flash intensities presumably because, in the absence of EGTA, Ca^{2+} could evoke release at neighboring InsP$_3$R clusters. Ca^{2+} puffs in non-buffered cells were evoked by low energy flash photolysis of a low concentration (6.25 μM) of caged InsP$_3$. In the representative cell, a single Ca^{2+} puff was evoked in response to photolysis of InsP$_3$ (Fig. 4). $[Ca^{2+}]_c$ was increased at this location by 0.88 $\Delta F/F_0$. The average puff amplitude in non-buffered myocytes was 1.01 ± 0.17 $\Delta F/F_0$ ($n = 3$). The average time to peak (10–90% interval) was 419 ± 141 ms, FWHD was 481 ± 76 ms, and the decay time (90–10% interval) was 1066 ± 279 ms (Table 1). The rise and decay of Ca^{2+} puffs from non-buffered cells were both slower than that measured in EGTA-buffered cells suggesting that EGTA facilitates diffusion of Ca^{2+} away from an InsP$_3$R cluster presumably by capturing the ion (37). Increasing the flash lamp intensity, which liberates a greater amount of InsP$_3$, triggered a global rise in Ca^{2+} (Fig. 4). The global $[Ca^{2+}]_c$ increase, evoked by the greater release of InsP$_3$, was 3.48 $\Delta F/F_0$.

To ensure Ca^{2+} puffs arose from InsP$_3$-mediated Ca^{2+} release the effect of the InsP$_3$R blocker 2-aminoethoxydiphenyl borate (2-APB) was examined. In this series of experiments EGTA (300 μM) was again used to facilitate the measurement of consistent Ca^{2+} puffs. Approximately reproducible Ca^{2+} puffs were evoked by photolysis of caged InsP$_3$ (25 μM) (Fig. 5). Ca^{2+} puffs were abolished within 60 s by 2-APB (100 μM) (Fig. 5). Ca^{2+} puff amplitude was 2.04 ± 0.32 $\Delta F/F_0$ before and 0.25 ± 0.02 $\Delta F/F_0$ ($n = 3$) ($p < 0.05$) after application of 2-APB. Together these results suggest the localized Ca^{2+} increases evoked by InsP$_3$R in EGTA-buffered colonic myocytes are Ca^{2+} puffs and suitable for the examination of the influence of mitochondrial Ca^{2+} uptake on intra-cluster dynamics during InsP$_3$-mediated SR Ca^{2+} release.

Mitochondrial Control of Ca^{2+} Puffs—To determine whether or not mitochondria modulate InsP$_3$-mediated Ca^{2+} signaling by operating within or between InsP$_3$R clusters, the effect of inhibition of mitochondrial Ca^{2+} uptake on Ca^{2+} puffs was examined. The slow Ca^{2+} chelator EGTA (300 μM), as before, was used to prevent Ca^{2+} released from one InsP$_3$R

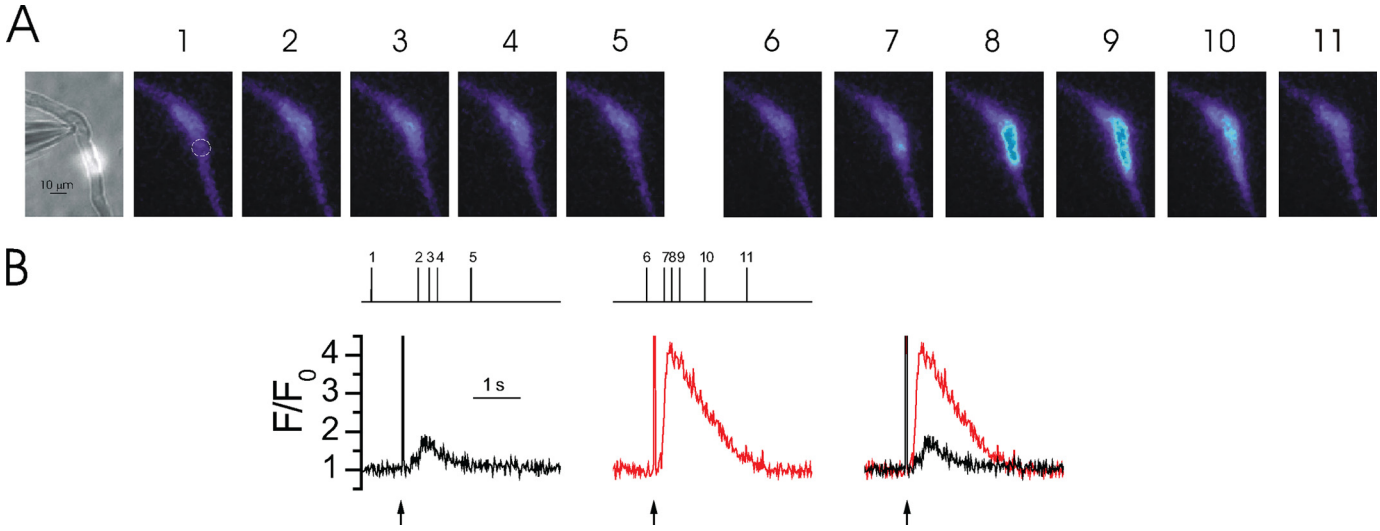

FIGURE 4. **InsP$_3$-mediated Ca^{2+} puffs and global Ca^{2+} increases.** At −70 mV, locally photolyzed caged InsP$_3$ (6.25 μM) (↑, *B*) in a ~20-μm diameter region (*A*, *bright spot* in *left-hand panel*, see also whole cell electrode, *left side*) evoked a Ca^{2+} puff that was preceded by a Ca^{2+}"blip"-like event (*A* and *B*). Flash photolysis of caged InsP$_3$ in the area is indicated by the *circle,* in *A* each ~60 s generated Ca^{2+} puffs (*B*, *black line*). When photolysis energy was increased to photolyze more InsP$_3$ a larger amount of Ca^{2+} release occurred throughout the region (*B*, *red line*). The Ca^{2+} puff was overlaid (*B*, *right panel*) for comparison. The [Ca^{2+}]$_c$ images (*A*) are derived from the time points indicated by the corresponding numbers in *B*. [Ca^{2+}]$_c$ changes in *A* are expressed by color: *dark blue*, low and *light blue*, high [Ca^{2+}]$_c$. Measurements were made from a 3 × 3 pixel box located at the center of each Ca^{2+} release event (not shown). The large increase in fluorescence at time 0 is the flash artifact.

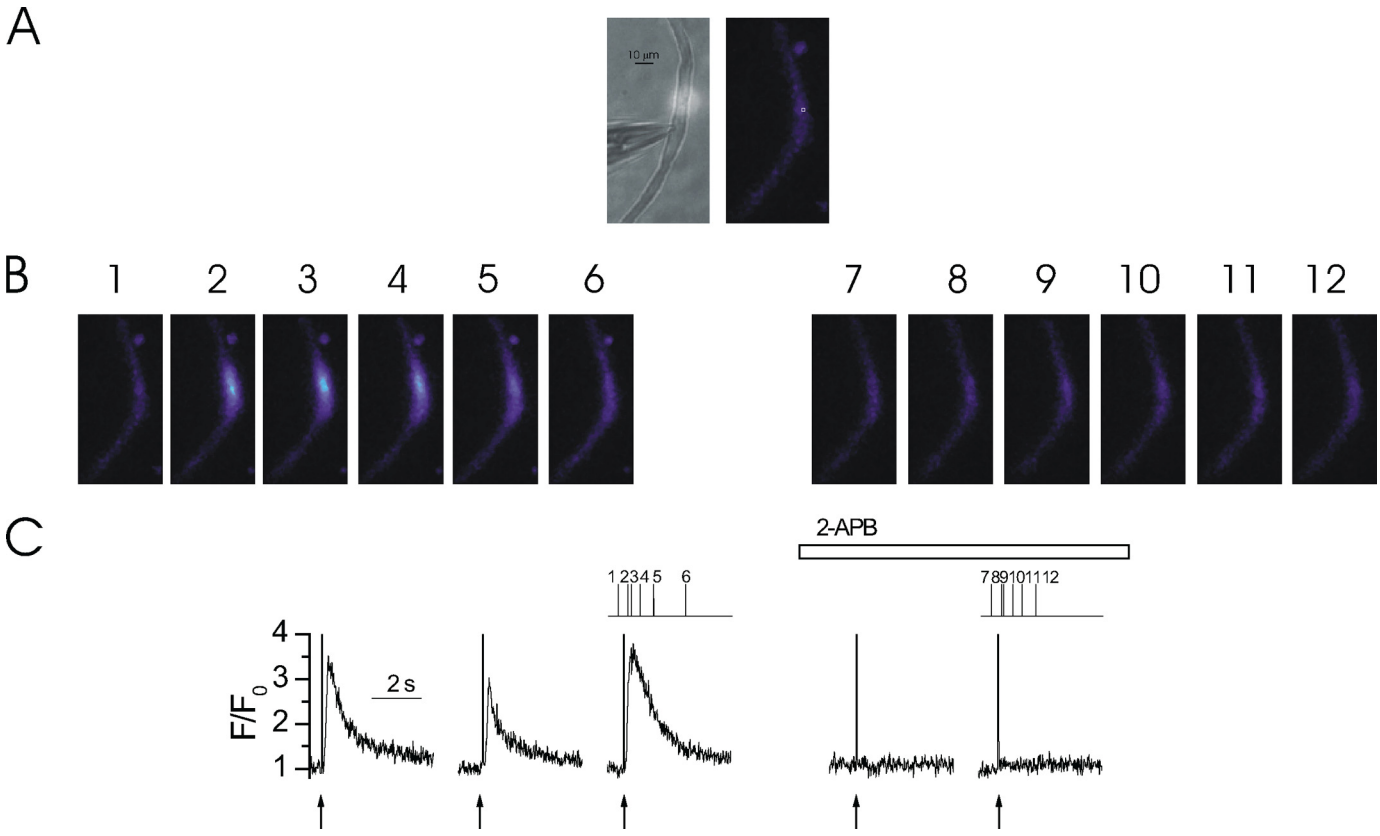

FIGURE 5. **Ca^{2+} puffs are inhibited by 2-APB.** At −70 mV, locally photolyzed caged InsP$_3$ (25 μM) (↑, *C*) in a ~20-μm diameter region (*A, bright spot* in *left-hand panel*, see also whole cell electrode, *left side*) evoked Ca^{2+} puffs in an EGTA (300 μM)-buffered colonic myocyte (*B* and *C*). A second and third photolysis of InsP$_3$, each at ~60-s intervals, at the same site generated an approximately comparable [Ca^{2+}]$_c$ increase (*C*). Superfusion of 2-APB (100 μM) abolished InsP$_3$-mediated Ca^{2+} puffs within ~60 s (*B* and *C*). The [Ca^{2+}]$_c$ images (*B*) are derived from the time points indicated by the corresponding numbers in *C*. [Ca^{2+}]$_c$ changes in *B* are represented by color: *dark blue*, low and *light blue*, high [Ca^{2+}]$_c$. Measurements were made from a 3 × 3 pixel box (*A*, *right-hand panel*, *white square*). The large increase in fluorescence at time 0 is the flash artifact.

cluster from activating neighboring InsP$_3$R clusters and generating a global Ca^{2+} rise. Ca^{2+} puffs were evoked by localized flash photolysis of caged InsP$_3$ at 60-s intervals (Fig. 6). When the cell was superfused with CCCP (1 μM; and oligomycin, 6 μM), to depolarize $\Delta\Psi_M$ and inhibit mitochondrial Ca^{2+} uptake, Ca^{2+} puff amplitude decreased to 34% of control

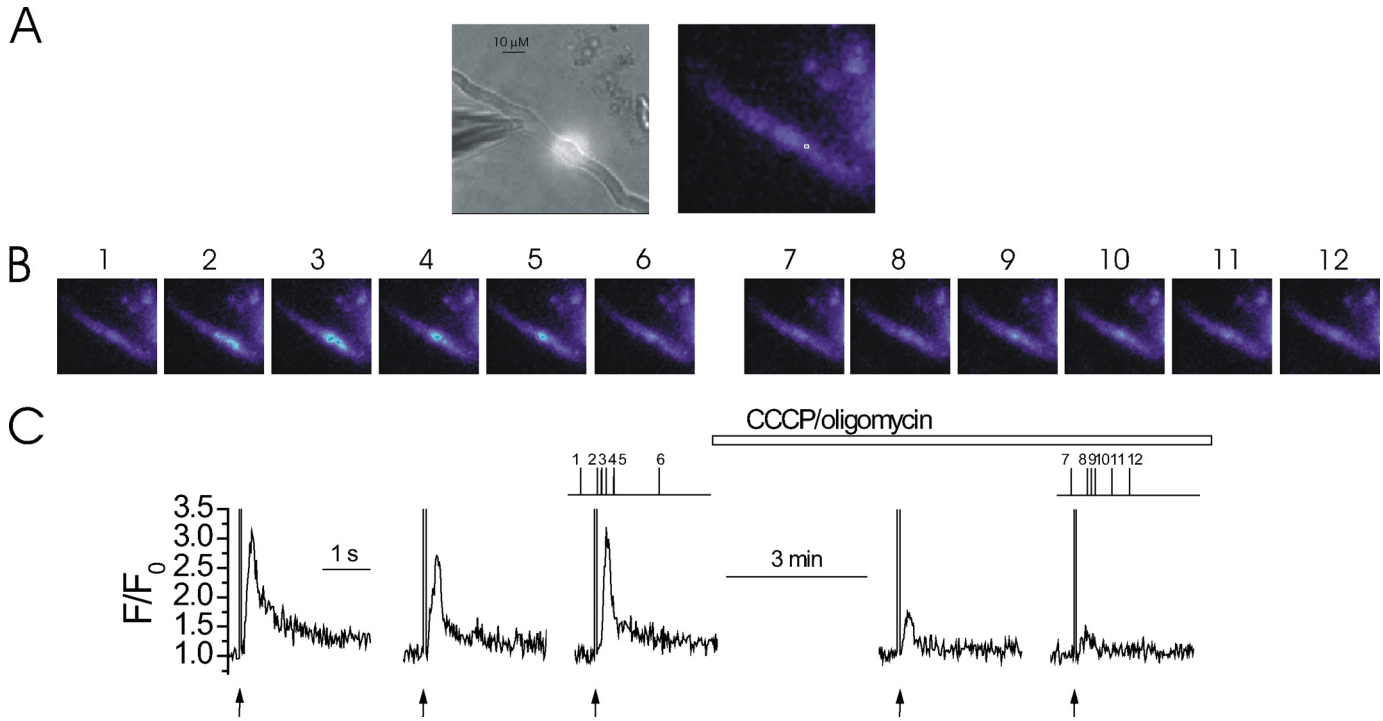

FIGURE 6. **Depolarization of $\Delta\Psi_M$ with CCCP/oligomycin inhibits Ca^{2+} puffs.** At −70 mV, locally photolyzed caged $InsP_3$ (25 μM) (↑, *C*) in a ~20-μm diameter region (*A*, *bright spot* in *left-hand panel*, see also whole cell electrode, *left side*) evoked Ca^{2+} puffs in an EGTA (300 μM)-buffered colonic myocyte (*B* and *C*). Note: there are two individual Ca^{2+} puff sites in response to photorelease of $InsP_3$; one site releases Ca^{2+} just before the other site. Flash photolysis of $InsP_3$ every ~60 s generated approximately comparable $[Ca^{2+}]_c$ increases (*C*). Superfusion of CCCP and oligomycin (1 and 6 μM, respectively) while continuing to photolyze $InsP_3$ at ~60 intervals, decreased the amplitude of $InsP_3$-mediated Ca^{2+} puffs (*B* and *C*). The $[Ca^{2+}]_c$ images (*B*) are derived from the time points indicated by the corresponding numbers in *C*. $[Ca^{2+}]_c$ changes in *B* are expressed by color: *dark blue*, low and *light blue*, high $[Ca^{2+}]_c$. Measurements were made from a 3 × 3 pixel box (*A*, *right-hand panel*, *white square*). The large increase in fluorescence at time 0 is the flash artifact.

(1.34 ± 0.17 $\Delta F/F_0$ before and 0.46 ± 0.05 $\Delta F/F_0$ after CCCP, $n = 5$, $p < 0.05$; Fig. 6). Rotenone (5 μM; and oligomycin, 6 μM) a complex 1 inhibitor, which also depolarizes the $\Delta\Psi_M$ and prevents mitochondrial Ca^{2+} uptake, inhibited SR Ca^{2+} release. Ca^{2+} puff amplitude was decreased to 40% of its original amplitude in rotenone (Fig. 7). Thus, Ca^{2+} puff amplitude was 2.02 ± 0.36 $\Delta F/F_0$ before and 0.82 ± 0.15 $\Delta F/F_0$ after rotenone application ($n = 4$, $p < 0.05$). Direct inhibition of mitochondrial Ca^{2+} uptake by Ru360 (10 μM) also inhibited Ca^{2+} puff amplitude to 38% of control values (from 1.32 ± 0.40 in control to 0.51 ± 0.03 in Ru360 $\Delta F/F_0$, $n = 9$ puffs from 3 cells, $p < 0.05$). These results suggest that Ca^{2+} released from a cluster of $InsP_3R$ is taken up by mitochondria before it diffuses to other neighboring clusters, *i.e.* mitochondrial Ca^{2+} uptake is involved in regulating $InsP_3R$ Ca^{2+} release at the intra-cluster level.

The results suggest that mitochondrial Ca^{2+} uptake prolongs Ca^{2+} release and occurs rapidly to influence the kinetics of Ca^{2+} release within an $InsP_3R$ cluster. To test this proposal further the cell was buffered with fast Ca^{2+} chelator BAPTA. Although BAPTA has a similar Ca^{2+} binding affinity to EGTA its faster binding kinetics (K_{on} = 100–1000 μM^{-1} s^{-1}) allows BAPTA to capture the ion while within an $InsP_3R$ cluster in a way similar to how mitochondrial Ca^{2+} uptake is proposed to function. A Ca^{2+} puff evoked in an EGTA-buffered myocyte is compared with a Ca^{2+} release event of the same magnitude in a BAPTA-buffered myocyte (Fig. 8). Although the average peak amplitude (1.53 ± 0.54 $\Delta F/F_0$ in BAPTA) was similar to that in EGTA, the average time to peak (1486 ± 156 ms; $n = 12$ from 4 cells), a measure of the time course of release, was significantly prolonged in BAPTA-buffered myocytes (Table 1). These results suggest that restricting the $[Ca^{2+}]_c$ change at an $InsP_3R$ cluster prolongs the time course of $InsP_3$-meditated Ca^{2+} release. These results are consistent with those in *Xenopus* oocytes; BAPTA prolonged the duration of $InsP_3$-mediated Ca^{2+} release and Ca^{2+} release events were no longer spatially discrete (28). This experiment further supports that mitochondrial Ca^{2+} uptake influences both global and local $InsP_3$-mediated Ca^{2+} signals.

DISCUSSION

$InsP_3$-sensitive Ca^{2+} release initiates at discrete sites on the SR. These sites contain a few tens of receptors from which the local increase in $[Ca^{2+}]$ is termed a puff. Ca^{2+} puffs are spatially restricted events and of short duration. Puffs are considered elementary release events and may interact and coalesce to generate a global release in Ca^{2+}. In the present study Ca^{2+} puffs, evoked by photorelease of caged $InsP_3$, occurred in multiple regions of the cell either near simultaneously or after various latencies of onset. Ca^{2+} puffs at different locations had various amplitudes and durations. Yet, at an individual site Ca^{2+} puff amplitude was relatively constant in response to a given $[InsP_3]$. Ca^{2+} puffs occurred by the release of Ca^{2+} from $InsP_3R$. In support, puffs were blocked by the $InsP_3R$ inhibitor 2-APB.

In smooth muscle, global $InsP_3$-mediated Ca^{2+} release is modulated by mitochondrial Ca^{2+} uptake. $InsP_3$-evoked Ca^{2+} release decreased when the driving force for mitochondrial Ca^{2+} uptake was collapsed by depolarization of $\Delta\Psi_M$ with

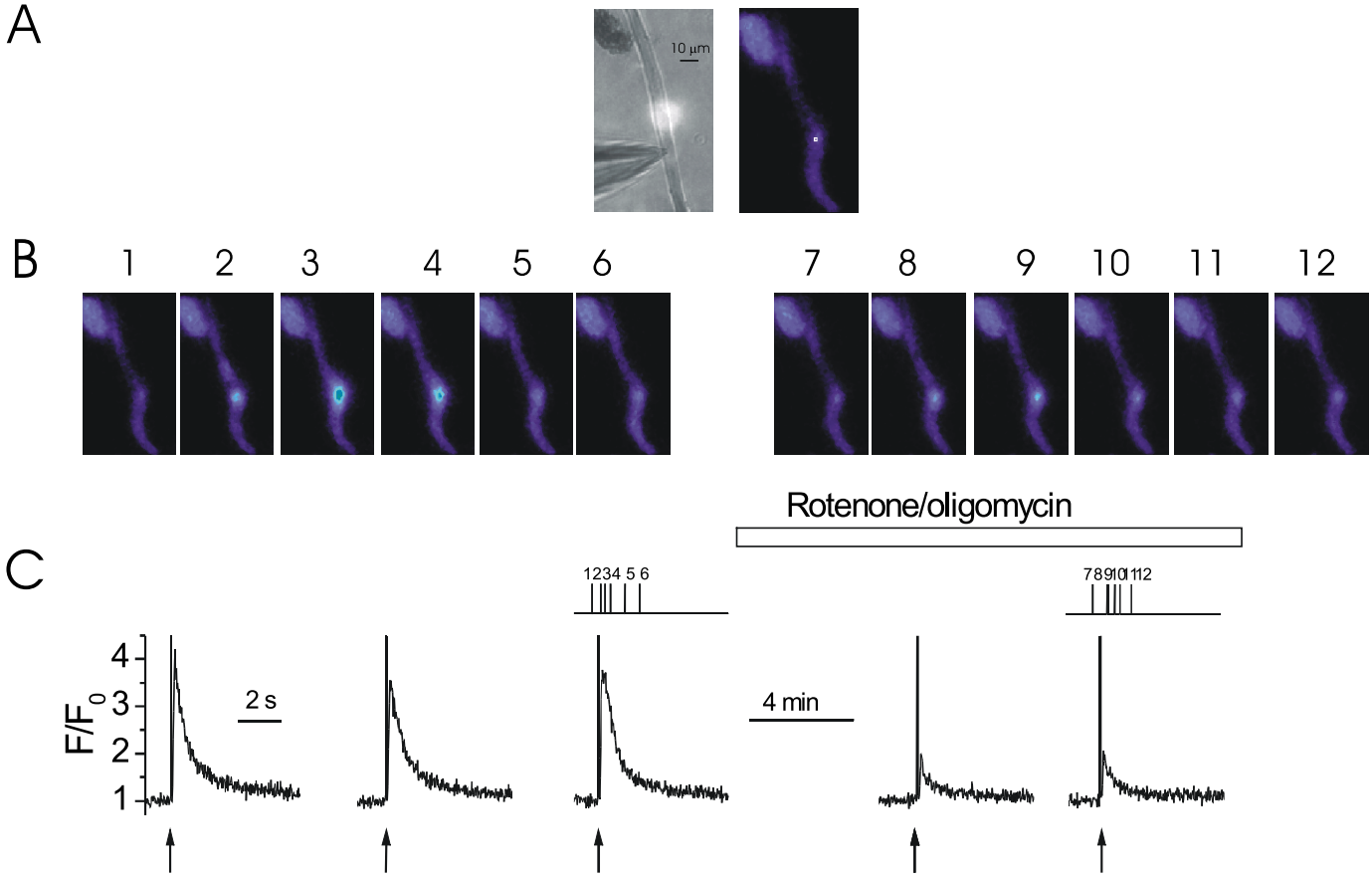

FIGURE 7. **Depolarization of $\Delta\Psi_M$ with rotenone inhibits Ca^{2+} puffs.** At −70 mV, locally photolyzed caged $InsP_3$ (25 μM) (↑, *C*) in a ~20-μm diameter region (*A*, *bright spot* in *left-hand panel*, see also whole cell electrode, *left side*) evoked Ca^{2+} puffs in an EGTA (300 μM)-buffered colonic myocyte (*B* and *C*). Flash photolysis of $InsP_3$ every ~60 s generated approximately comparable $[Ca^{2+}]_c$ increases (*C*). Superfusion of rotenone and oligomycin (5 and 6 μM, respectively), whereas continuing to photolyze $InsP_3$ at ~60-s intervals, decreased the amplitude of $InsP_3$-mediated Ca^{2+} puffs (*B* and *C*). The $[Ca^{2+}]_c$ images (*B*) are derived from the time points indicated by the corresponding numbers in *C*. $[Ca^{2+}]_c$ changes in *B* are expressed by color: *dark blue*, low and *light blue*, high $[Ca^{2+}]_c$. Measurements were made from a 3 × 3 pixel box (*A*, *right-hand panel*, *white square*). The large increase in fluorescence at time 0 is the flash artifact.

either CCCP or rotenone (15, 16, 25). How mitochondria regulate $InsP_3$-mediated Ca^{2+} signals was examined here. If Ca^{2+} uptake occurred at an $InsP_3R$ cluster mitochondria would influence local Ca^{2+} signaling at the level of a puff. Alternatively, if Ca^{2+} uptake occurred between clusters then mitochondria would influence global but not local Ca^{2+} signals. These two possibilities were addressed by examining the influence of mitochondria on local Ca^{2+} signals. When mitochondrial Ca^{2+} uptake was prevented by depolarizing $\Delta\Psi_M$ with CCCP or rotenone, Ca^{2+} puff amplitude decreased by 66 or 60%, respectively. When mitochondrial Ca^{2+} uptake was prevented directly by the uniporter antagonist Ru360, Ca^{2+} puff amplitude decreased by 62%. These results suggest that mitochondria regulate Ca^{2+} release by acting within an IP_3R cluster.

Ca^{2+} exerts positive and negative feedback effects on IP_3R. Positive feedback, which increases Ca^{2+} release, occurs over lower concentrations of the ion (~<500 nM), whereas negative feedback dominates at higher $[Ca^{2+}]$. Mitochondria because of their low affinity for the ion may limit only the negative feedback effect of Ca^{2+} on the IP_3-mediated Ca^{2+} release. In support of the occurrence of negative feedback the fast Ca^{2+} chelator BAPTA prolonged Ca^{2+} release in a way similar to how mitochondrial Ca^{2+} uptake appears to function to increase the $InsP_3$-mediated Ca^{2+} release. Together the results suggest mitochondrial Ca^{2+} uptake influences the amount of Ca^{2+} released from a cluster of $InsP_3R$ and as a result will regulate both local and global $InsP_3$-mediated Ca^{2+} signals.

The question arises as to how mitochondria, by lowering $[Ca^{2+}]$ near IP_3R, increases the $[Ca^{2+}]_c$ derived from IP_3R activity. Large increases in $[Ca^{2+}]_c$ (~1 μM) may generate a persistent reduction in activity in IP_3R, which resembles channel inactivation (29, 40). When IP_3R falls into this inactivated-like state Ca^{2+} release is terminated for many (up to 30) seconds (29, 40). Mitochondria by removing Ca^{2+} near IP_3R may prevent the ion from reaching a concentration high enough to induce the persistent inactivation of the channel. Ca^{2+} release may persist when mitochondria maintain a slightly lower $[Ca^{2+}]$ near IP_3R.

Other support for close proximity between sites of mitochondrial Ca^{2+} uptake and sites of SR Ca^{2+} release has come predominantly from experiments that measure increases in both $[Ca^{2+}]_c$ and mitochondrial Ca^{2+} concentration ($[Ca^{2+}]_{mit}$) during $InsP_3$-mediated Ca^{2+} release (11, 17, 18, 41). In rat basophilic leukemia-2H3 mast cells buffering $[Ca^{2+}]_c$ with EGTA (100 μM) decreased the global $[Ca^{2+}]_c$ signal yet did not prevent an increase in $[Ca^{2+}]_{mit}$ (22). This result suggests that $InsP_3R$ clusters are located to within 100 nm of sites of mitochondrial Ca^{2+} uptake. It may be that there are structural

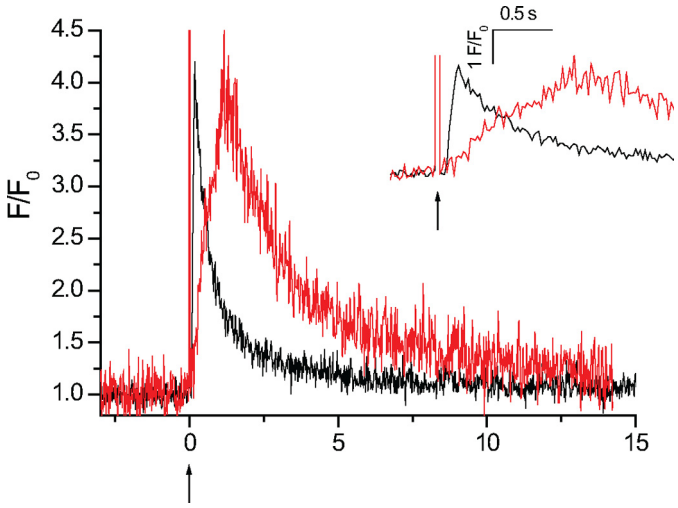

FIGURE 8. **Localized $InsP_3$-mediated Ca^{2+} release in BAPTA- and EGTA-buffered myocytes.** When myocytes are buffered with the fast Ca^{2+} chelator BAPTA, Ca^{2+} release is significantly prolonged. A Ca^{2+} puff in an EGTA (300 μM)-buffered myocyte (*black trace*) is compared with a Ca^{2+} release event of a comparable magnitude in a BAPTA (250 μM)-buffered myocyte (*red trace*). Myocytes were voltage-clamped at −70 mV and caged $InsP_3$ (25 μM) (↑) was locally photolyzed in a ~20-μm diameter region (not shown). The rate of rise, a measure of the time course of Ca^{2+} release, was significantly increased when compared with an EGTA-buffered myocyte. The *inset* shows an expanded time scale to illustrate the differences in rate of rise of the Ca^{2+} events in the EGTA (*black line*)- and BAPTA (*red line*)-buffered myocytes. Measurements were made from 3 × 3 pixel boxes located at the center of each Ca^{2+} release event (not shown). The large increase in fluorescence at time 0 is the flash artifact.

tethers that keep sites of mitochondrial Ca^{2+} uptake and SR Ca^{2+} release in close proximity (42). Indeed, structural evidence provides support for close association between mitochondria and SR membranes. Close associations between the SR and mitochondrial membranes have been noted in several cell types (21, 22, 43–45). For example, in unstimulated tracheal smooth muscle the majority of mitochondria completely enveloped and form multiple junctions with at least one contact point within ~22 nm of the SR (43, 45). In HeLa cells there are also close contacts between the endoplasmic reticulum and mitochondria (5–20% mitochondrial surface) (21). Immunogold labeling of thin sections of Purkinje neurons demonstrated close associations between mitochondria and $InsP_3R$ in stacked endoplasmic reticulum cisternae (46, 47). It is in these regions of close contact that Ca^{2+} released from the SR is proposed to be taken up by mitochondria via the Ca^{2+} uniporter (11, 48).

Although there is close proximity between SR and mitochondria, Ca^{2+} uptake may either positively or negatively regulate local $InsP_3$-mediated Ca^{2+} release. In oligodendrocyte progenitor cells, as in the present study, mitochondrial Ca^{2+} uptake positively affected (increased) $InsP_3$-mediated Ca^{2+} release. Depolarizing $\Delta\Psi_M$ decreased the number of cells that exhibited methacholine-evoked Ca^{2+} puffs and shortened the duration of Ca^{2+} puffs in those cells that still responded (49). However, the changes in puff characteristics were attributed to a decrease in the amount of agonist-mediated $InsP_3$ produced after $\Delta\Psi_M$ depolarization rather than feedback regulation of $InsP_3R$ activity. Changes in $InsP_3$ concentration are an unlikely explanation for the present findings in smooth muscle because the concentration of inositide was increased by photolysis of caged $InsP_3$ rather than being generated by an agonist.

Alternatively, there may be a negative relationship between mitochondrial function and Ca^{2+} puff amplitude when $InsP_3R$ clusters are in close proximity to sites of mitochondrial Ca^{2+} uptake. In rat basophilic leukemia-2H3 mast cells, although sites of mitochondrial Ca^{2+} uptake are located near $InsP_3R$, inhibition of mitochondrial Ca^{2+} uptake increased $InsP_3$-mediated Ca^{2+} release (22). In *Xenopus* oocytes the majority of mitochondria are located an average of ~2.3 μm from Ca^{2+} puffs sites so that they are separated by a distance where presumably they do not take up Ca^{2+} during a Ca^{2+} puff (44). Yet, there are also a small subset of mitochondria that are in close proximity (<1.25 μm) to Ca^{2+} release sites. Upon sustained $InsP_3$ application, both Ca^{2+} puffs and Ca^{2+} wave initiation occurred less frequently at sites where mitochondria were in close proximity to the SR suggesting that this population of mitochondria function to prevent Ca^{2+} release (*i.e.* mitochondria support a negative feedback influence of $InsP_3$-mediated Ca^{2+} release) (44). Interestingly, the amplitude of the global $InsP_3$-evoked Ca^{2+} response decreased when mitochondrial Ca^{2+} uptake was prevented in *Xenopus* oocytes (*i.e.* in this case mitochondria appear to provide a positive feedback influence on Ca^{2+} release) (20). Initially, the effects of mitochondria on local and global signals may appear contradictory. Perhaps in *Xenopus* oocytes mitochondria may influence inter-cluster (positive feedback) as well as intra-cluster (negative feedback) communication.

Both the positive and negative effects of $\Delta\Psi_M$ depolarization on $InsP_3$-mediated Ca^{2+} release were prevented when cells were buffered using BAPTA (23, 39). These results suggest mitochondrial effects on $InsP_3$-mediated Ca^{2+} release are exerted via Ca^{2+} uptake. For example, uncoupling $InsP_3R$ clusters with BAPTA prevented the potentiation of $InsP_3$-mediated Ca^{2+} release, which occurred upon depolarizing $\Delta\Psi_M$ in hepatocytes (23). BAPTA also restored $InsP_3$-mediated Ca^{2+} release, which had decreased after depolarizing $\Delta\Psi_M$ in baby hamster kidney-21 cells (39). In the present study BAPTA prolonged $InsP_3$-mediated Ca^{2+} release. In both smooth muscle and *Xenopus* oocytes BAPTA appears to operate by binding to Ca^{2+} within an $InsP_3R$ cluster and preventing intra-cluster negative feedback to prolong the SR Ca^{2+} release (28). At the concentration used (250 μM) BAPTA should "capture" Ca^{2+} ~70–200 nm from the release site (28). Thus BAPTA, which both prolongs $InsP_3$-mediated Ca^{2+} release and prevents $\Delta\Psi_M$ depolarization from affecting $InsP_3$-mediated Ca^{2+} release, supports a direct role of mitochondrial Ca^{2+} uptake in influencing $InsP_3R$ communication at the intra-cluster level.

In conclusion, in colonic smooth muscle sites of mitochondrial Ca^{2+} uptake influence $InsP_3$-mediated Ca^{2+} release within an $InsP_3R$ cluster. Presumably close contacts between mitochondria and $InsP_3R$ act to prevent negative feedback inhibition of Ca^{2+} release at $InsP_3R$ clusters. The interaction between mitochondria and SR will modulate Ca^{2+} signaling mechanisms from local Ca^{2+} puffs to global Ca^{2+} oscillations and waves.

REFERENCES

1. Taylor, C. W., and Laude, A. J. (2002) *Cell Calcium* **32,** 321–334
2. Iino, M. (1990) *J. Gen. Physiol.* **95,** 1103–1122

3. Bezprozvanny, I., Watras, J., and Ehrlich, B. E. (1991) *Nature* **351,** 751–754
4. Swillens, S., Dupont, G., Combettes, L., and Champeil, P. (1999) *Proc. Natl. Acad. Sci. U.S.A.* **96,** 13750–13755
5. Shuai, J., Rose, H. J., and Parker, I. (2006) *Biophys. J.* **91,** 4033–4044
6. Parker, I., and Yao, Y. (1991) *Proc. Biol. Sci.* **246,** 269–274
7. Bootman, M., Niggli, E., Berridge, M., and Lipp, P. (1997) *J. Physiol.* **499,** 307–314
8. Bootman, M. D., Berridge, M. J., and Lipp, P. (1997) *Cell* **91,** 367–373
9. Yao, Y., Choi, J., and Parker, I. (1995) *J. Physiol.* **482,** 533–553
10. Boittin, F. X., Coussin, F., Morel, J. L., Halet, G., Macrez, N., and Mironneau, J. (2000) *Biochem. J.* **349,** 323–332
11. Rizzuto, R., Brini, M., Murgia, M., and Pozzan, T. (1993) *Science* **262,** 744–747
12. Horne, J. H., and Meyer, T. (1997) *Science* **276,** 1690–1693
13. Sun, X. P., Callamaras, N., Marchant, J. S., and Parker, I. (1998) *J. Physiol.* **509,** 67–80
14. Parker, I., and Yao, Y. (1996) *J. Physiol.* **491,** 663–668
15. Chalmers, S., and McCarron, J. G. (2008) *J. Cell Sci.* **121,** 75–85
16. McCarron, J. G., and Muir, T. C. (1999) *J. Physiol.* **516,** 149–161
17. Simpson, P. B., and Russell, J. T. (1996) *J. Biol. Chem.* **271,** 33493–33501
18. Drummond, R. M., and Tuft, R. A. (1999) *J. Physiol.* **516,** 139–147
19. Collins, T. J., Lipp, P., Berridge, M. J., Li, W., and Bootman, M. D. (2000) *Biochem. J.* **347,** 593–600
20. Jouaville, L. S., Ichas, F., Holmuhamedov, E. L., Camacho, P., and Lechleiter, J. D. (1995) *Nature* **377,** 438–441
21. Rizzuto, R., Pinton, P., Carrington, W., Fay, F. S., Fogarty, K. E., Lifshitz, L. M., Tuft, R. A., and Pozzan, T. (1998) *Science* **280,** 1763–1766
22. Csordás, G., Thomas, A. P., and Hajnóczky, G. (1999) *EMBO J.* **18,** 96–108
23. Hajnóczky, G., Hager, R., and Thomas, A. P. (1999) *J. Biol. Chem.* **274,** 14157–14162
24. Boitier, E., Rea, R., and Duchen, M. R. (1999) *J. Cell Biol.* **145,** 795–808
25. Swärd, K., Dreja, K., Lindqvist, A., Persson, E., and Hellstrand, P. (2002) *Circ. Res.* **90,** 792–799
26. Bradley, K. N., Flynn, E. R., Muir, T. C., and McCarron, J. G. (2002) *J. Physiol.* **538,** 465–482
27. Callamaras, N., and Parker, I. (2000) *EMBO J.* **19,** 3608–3617
28. Dargan, S. L., and Parker, I. (2003) *J. Physiol.* **553,** 775–788
29. McCarron, J. G., MacMillan, D., Bradley, K. N., Chalmers, S., and Muir, T. C. (2004) *J. Biol. Chem.* **279,** 8417–8427
30. McCarron, J. G., Craig, J. W., Bradley, K. N., and Muir, T. C. (2002) *J. Cell Sci.* **115,** 2207–2218
31. MacMillan, D., Chalmers, S., Muir, T. C., and McCarron, J. G. (2005) *J. Physiol.* **569,** 533–544
32. McCarron, J. G., and Olson, M. L. (2008) *J. Biol. Chem.* **283,** 7206–7218
33. McCarron, J. G., Chalmers, S., and Muir, T. C. (2008) *J. Cell Sci.* **121,** 86–98
34. Parker, I., and Yao, Y. (1995) *Ciba Found. Symp.* **188,** 50–60; discussion 60–55
35. Marchant, J. S., and Parker, I. (1998) *Biochem. J.* **334,** 505–509
36. Rose, H. J., Dargan, S., Shuai, J., and Parker, I. (2006) *Biophys. J.* **91,** 4024–4032
37. Smith, I. F., Wiltgen, S. M., and Parker, I. (2009) *Cell Calcium* **45,** 65–76
38. Thomas, D., Lipp, P., Berridge, M. J., and Bootman, M. D. (1998) *J. Biol. Chem.* **273,** 27130–27136
39. Landolfi, B., Curci, S., Debellis, L., Pozzan, T., and Hofer, A. M. (1998) *J. Cell Biol.* **142,** 1235–1243
40. Oancea, E., and Meyer, T. (1996) *J. Biol. Chem.* **271,** 17253–17260
41. Hajnóczky, G., Robb-Gaspers, L. D., Seitz, M. B., and Thomas, A. P. (1995) *Cell* **82,** 415–424
42. Csordás, G., Renken, C., Várnai, P., Walter, L., Weaver, D., Buttle, K. F., Balla, T., Mannella, C. A., and Hajnóczky, G. (2006) *J. Cell Biol.* **174,** 915–921
43. Dai, J., Kuo, K. H., Leo, J. M., van Breemen, C., and Lee, C. H. (2005) *Cell Calcium* **37,** 333–340
44. Marchant, J. S., Ramos, V., and Parker, I. (2002) *Am. J. Physiol. Cell Physiol.* **282,** C1374–C1386
45. Nixon, G. F., Mignery, G. A., and Somlyo, A. V. (1994) *J. Muscle Res. Cell Motil.* **15,** 682–700
46. Satoh, T., Ross, C. A., Villa, A., Supattapone, S., Pozzan, T., Snyder, S. H., and Meldolesi, J. (1990) *J. Cell Biol.* **111,** 615–624
47. Mignery, G. A., Südhof, T. C., Takei, K., and De Camilli, P. (1989) *Nature* **342,** 192–195
48. Rizzuto, R., Bastianutto, C., Brini, M., Murgia, M., and Pozzan, T. (1994) *J. Cell Biol.* **126,** 1183–1194
49. Haak, L. L., Grimaldi, M., Smaili, S. S., and Russell, J. T. (2002) *J. Neurochem.* **80,** 405–415